

# Real-Time Discharge/Charge Rate Management for Hybrid Energy Storage in Electric Vehicles

Eugene Kim and Kang G. Shin

Department of Electrical Engineering and Computer Science  
The University of Michigan – Ann Arbor, U.S.A.  
{kimsun,kgshin}@umich.edu

Jinkyu Lee

Department of Computer Science and Engineering  
Sungkyunkwan University, Republic of Korea  
jinkyu.lee@skku.edu

**Abstract**—Electric vehicles (EVs) are usually powered by a large number of battery cells, necessitating an effective battery management system (BMS) which protects the battery cells from harsh conditions while providing the required power efficiently. The discharge/charge rate of battery cells affects their health significantly, and existing BMSes employ simple discharge/charge rate scheduling so as to prevent weak cells from being discharged/charged excessively.

In this paper, we design and evaluate the real-time management of battery discharge/charge rate to extend the life of batteries in powering EVs based on their physical dynamics and operation history. We first explore a contemporary energy storage system for EVs to capture its physical dynamics that affect the battery discharge/charge rate; for example, a regenerative braking system for reusing the dissipated energy leads to current surges into the batteries, which shortens battery life. Based on understanding of the effects of discharge/charge rate in an energy storage system, we first devise control knobs for manipulating the discharge/charge rate. Then, we design an *adaptive* algorithm that manages the discharge/charge rate by determining the control knobs with a *reconfigurable* energy storage architecture. Our in-depth evaluation demonstrates that the proposed discharge/charge rate management improves battery life up to 37.7% at little additional cost compared to the existing energy storage systems.

## I. INTRODUCTION

Electric vehicles (EVs) are gaining popularity for their environmental friendliness and potential economic benefit. However, EVs have not yet dominated the internal combustion engine vehicles in the market due mainly to their high price resulting from high battery cost. Thus, the EV manufacturers have been focusing on the reduction of battery cost to increase their market share. For example, Tesla Motors recently announced a plan to invest up to 5 billion dollars through 2020 to produce cheaper batteries for EVs via mass production [1].

An effective battery management system (BMS) can reduce the required number of battery cells and extend the replacement period, hence reducing the battery cost. As part of our goal of designing such a BMS, we will in this paper focus on extending batteries' life which has significant impact on the battery cost. *Battery life* is defined as the duration (measured in the number of cycles or elapsed time) of a rechargeable battery until it degrades irreversibly and cannot hold a useful capacity of the underlying applications [2]. That is, the battery capacity monotonically decreases with time, and will never be recovered. As a result, EVs must be equipped with enough batteries to maintain the required capacity throughout their

warranty period. This capacity degradation may also require battery replacements, incurring an additional (maintenance) cost. It is therefore necessary for the BMS to slow down the capacity degradation of batteries in order to reduce the cost of purchasing and maintaining EVs.

Among the various reasons for battery capacity degradation, the discharge/charge rate is reported to be the most critical [3,4]. For example, a continuous exposure to high discharge current leads to fast capacity degradation, thereby shortening the battery life [5,6], which is inevitable due to abrupt changes in the EVs' power requirement, such as acceleration. To extend the battery life, researchers focused on hybrid energy storage systems (HESSes) built with two or more types of energy storage devices [7–11]. The main principle for regulating the battery' discharge/charge rate in a HESS is to adjust the discharge/charge rate for each storage device.

The goal of this paper is, therefore, to develop discharge/recharge rate management for an efficient HESS so as to reduce its initial deployment and maintenance costs. It requires not only comprehensive understanding of physical dynamics beneath the HESS, but also efficient management of the HESS based on this understanding. For example, in a HESS consisting of batteries, ultra-capacitors (UCs) and boost-buck DC/DC converters, the discharge/charge rate of each storage is dominated by a second-order differential equation, and we have to carefully regulate the parameters in the equation so as to minimize battery performance degradation. That is, we need to take a *cyber-physical perspective*, integrating and coordinating physical dynamics and adaptive controls as follows. First, we capture parameters affecting the discharge/charge rate in the HESS based on the circuit dynamics that represent the underlying discharge/charge operations. Second, we introduce three key control knobs that can manipulate the parameters, and develop management algorithms that manipulate control knobs to extend battery life using *adaptive* control schemes. Finally, we propose a *reconfigurable* architecture that realizes our management algorithms to regulate control knobs.

We evaluate the proposed battery discharge/charge rate management using workloads based on real driving patterns, and simulate them with a popular simulation tool. Our evaluation results demonstrate the effectiveness of the proposed battery discharge/charge rate management. Compared to the existing simple management schemes, our system improves the battery life up to 37.7% without increasing initial cost.

The main contributions of this paper are:

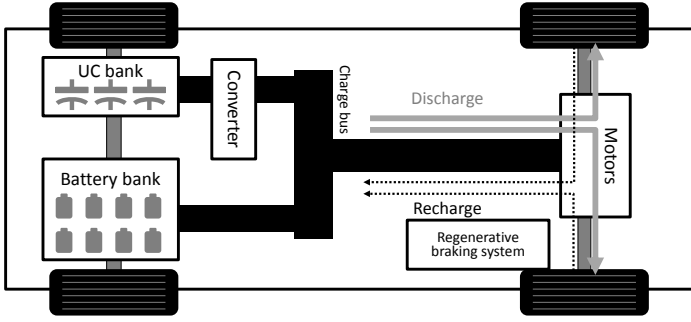


Fig. 1. Energy storage system in EVs

- Consideration of physical circuit dynamics to address the issues associated with battery life;
- Design of battery discharge/charge rate management with a new architecture; and
- In-depth, realistic evaluation of the HESS managements, demonstrating that the proposed system significantly increases the HESS efficiency without increasing initial cost.

The paper is organized as follows. Section II examines the state-of-art BMSes, each consisting of a regenerative braking system, batteries and UCs. Section III states the problem from a cyber-physical perspective. Section IV describes the physical dynamics related to the discharge/charge rate of batteries in a HESS. Section V presents our battery discharge/charge rate management algorithms, and Section VI describes a HESS management architecture. Section VII evaluates our system via simulation, and finally, the paper concludes with Section VIII.

## II. STATE-OF-ART BATTERY MANAGEMENT SYSTEMS

This section introduces the background of HESSes, including a brief review of existing BMSes. First, we describe the function and structure of a BMS shown in Fig. 1. Then, we introduce the part of a BMS that can supply power. Finally, we present an advanced architecture that can be incorporated into a BMS so as to overcome some disadvantages of existing simple BMSes; this architecture is the basis for our approach described in the following sections.

### A. Overview of BMS

As illustrated in Fig. 2, the power requirement of an EV is high and changes abruptly [8, 12, 13], because drivers frequently accelerate/decelerate their vehicles that weigh at least one ton during driving. Therefore, the battery management system (BMS) in an EV is responsible for providing motors with the required power while protecting battery cells from damage and life reduction caused by *short bursts of power transfer*. To perform such functions, a BMS is often comprised of two parts: (i) a large number of battery cells that can supply high current (hundreds of ampere) with high output voltage (tens or hundreds of volt), and (ii) an auxiliary system to mitigate the stress caused by large and abrupt power requirements from a regenerative braking system and motors.

### B. Regenerative braking system (RBS)

To meet the requirements of a BMS, most EVs are equipped with a regenerative braking system (RBS) to reuse

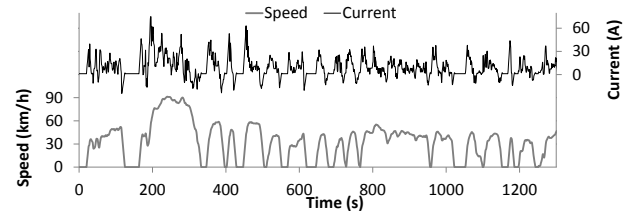


Fig. 2. Variation of an EV's power requirement

the energy dissipated in their braking system. During braking, the RBS converts the vehicle's kinetic energy to electrical energy that can be stored in batteries for reuse to power the vehicle. Its effectiveness has been substantiated in terms of fuel economy [14–17]. Although the RBS improves the utilization of energy, high recharging current for a very short period of time has a negative impact on the battery's health. Therefore, researchers deployed an auxiliary system that will be introduced next.

### C. Hybrid Energy Storage System (HESS)

Battery health is damaged by short bursts of discharging current supplied to motors and recharging current generated from the RBS. To remedy this problem, researchers deployed ultra-capacitors (UCs) in the BMS; a BMS with UCs as well as batteries is called a *hybrid energy storage system* (HESS). In a HESS, UCs are used as an energy buffer to smooth rapid power fluctuations in and out of the battery of an EV [18–21]. HESSes effectively utilize the properties of batteries and UCs, called *power density* and *energy density*. That is, available power density of batteries is lower than UCs so that the higher the discharge rate, the less efficient the energy conversion, whereas UCs do not suffer such efficiency degradation. On the other hand, UCs have lower energy density and higher unit cost than batteries as shown in Table I, implying that we should place a large number of UCs in an EV. Therefore, HESSes make batteries supply the average power required for operating vehicles, while UCs provide the sudden power surges required for acceleration and also accommodate instantaneous regenerative energy from the RBS.

Type	Ultra-capacitor	Lithium battery
Power density (W/kg)	100 - 10 K	80-2000
Energy density (WH/Kg)	1 - 10	60 - 150
Cost (USD/WH)	10.3	3.7

TABLE I. POWER DENSITY, ENERGY DENSITY, AND COST OF ENERGY STORAGEES [9]

Fig. 3 shows a simple HESS where an UC is connected directly to a battery, and the UC acts as a low pass filter so as to reduce the peak discharge current of the battery. Unfortunately, the HESS with this configuration requires a large number of UCs because the configuration cannot fully exploit UCs' capacity because of the same terminal voltages of the UC and the battery [19, 22]. To address this problem, many configurations of HESSes have been proposed [19, 20]. For example, Fig. 4 illustrates the most widely-studied configuration of HESS that includes a bi-directional DC/DC converter between a battery and an UC. This configuration allows voltage separation and an increase in utilization of the UC via the converter so as to reduce the required capacitance

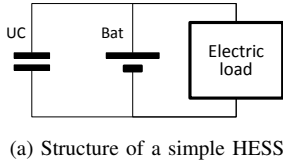


Fig. 3. A simple HESS

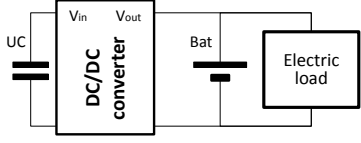


Fig. 4. A HESS with a DC/DC converter

(8F) of the UC in comparison with that (80F) of the simple HESS shown in Fig. 3.

#### D. Effective utilization of energy capacity for UCs in a HESS

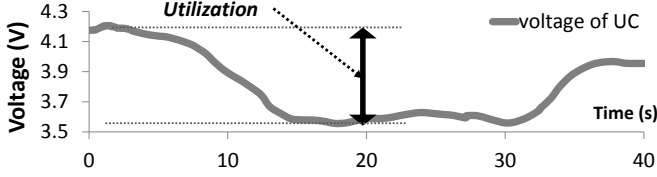


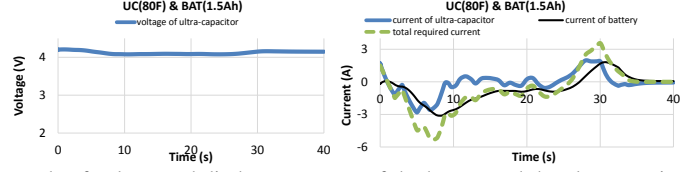
Fig. 5. Capacity utilization of a HESS

The ability of effectively utilizing UCs is a main focus in evaluating HESS configurations. That is, if we capture as much redundant energy into the UC bank as possible and then use all of that energy when required, we can efficiently utilize UCs without wasting the UC banks' capacity and their deployment cost. We can evaluate the utilization based on the law of storage in a standard capacitor. Energy stored in an UC ( $E_{UC}$ ) is affected by the voltage ( $V$ ) and the size of capacitors ( $C$ ) as:

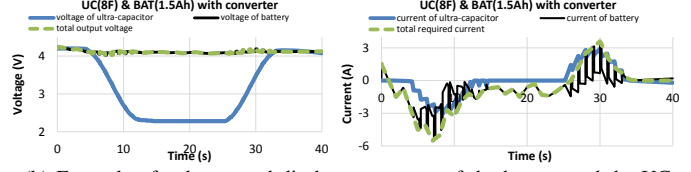
$$E_{UC} = \frac{1}{2}CV^2.$$

Therefore, the utilization of UCs' capacity can be measured by the range of voltage swing as shown in Fig. 5. For example, when 50% of an UC's voltage variation within a tolerable voltage range is permitted, 75% of the UC's energy can be delivered, whereas we can use only 20% of the energy for a 10% variation range, decreasing the UC's effectiveness. The HESS with a DC/DC converter in Fig. 4 shows high utilization of UCs' energy capacity by separating the voltage between the UC and the battery, while the simple HESS in Fig. 3 could not effectively utilize the energy capacity of UCs because the voltage drop is only 20%. To enhance the UCs' capacity utilization, several feedback control schemes have been proposed based on the UC-converter-battery architecture that regulates the discharge current adaptively [7, 10, 11, 19, 20].

Although a HESS can reduce the stresses and enhance the life of batteries, it still has not been used widely in commercial EVs, because UCs are not only expensive, but also required to endure high discharge current and high operating voltage. Furthermore, it takes a long time to find the optimal configuration for EVs, since it requires a number of tests in various environments. This is because discharge/charge current



(b) Example of voltage and discharge currents of the battery and the ultra capacitor (UC)



(b) Example of voltages and discharge currents of the battery and the UC

varies with driving conditions and behaviors which are related to a complex human decision-making process [13]. We will address these issues using adaptive control of converters and dynamic reconfiguration of UC banks.

### III. PROBLEM STATEMENT AND SOLUTION APPROACH

We want to develop a "good" HESS using an efficient and reliable BMS. We first introduce relevant terms and design constraints, state the problem, and then briefly describe our solution approach.

#### A. Battery life

A long lifetime of batteries reduces their number and extends their replacement periods, reducing the cost of EVs. Therefore, most BMSes are required to maintain appropriate battery operational environments to avoid damage and fast capacity reduction [23]. The battery life is known to depend on the number of discharge/charge cycles, the amount of energy used at each cycle (depth of discharge), operational temperature, and discharge/charge current [5, 6, 24–29]. Here we focus on the impact of discharge/charge current on the battery life, and propose a HESS that reduces stress of batteries, and doesn't affect the depth of discharge, operational temperature, and the number of cycles. Given the depth of discharge, operation cycle and operational temperature, the battery life depends on discharge current the battery supply as [5, 6]:

$$L_{cycle} = \alpha e^{-\beta I_{bat}}, \quad (1)$$

where  $L_{cycle}$  is the cycle life,  $I_{bat}$  is the discharge current,  $\alpha$  and  $\beta$  are positive coefficients. That is, a decrease in discharge/charge stress can extend the battery life exponentially.

#### B. Physical constraints and cost of components

To operate the electric motors satisfying vehicles' required drivability, a BMS is required to provide a large amount of charge in a few seconds. It should also maintain tolerable voltage and current for electric components during operation. The *rated voltage* ( $V_r$ ) of an UC is the maximum voltage that the UC is designed for. That is, to use UCs without destruction, we should keep UCs to operate within the tolerable voltage range. Likewise, we have to maintain the rated current when we use the converter. *Rated current* ( $I_r$ ) is defined as "the maximum amount of electrical current a device can carry

before sustaining immediate or progressive deterioration” [30]. From the market [31], we can acquire a variety of capacitors and converters, and the price depends on their specifications. Obviously, the larger capacitance or rated voltage, the more expensive. For example, an UC with 5.4V of rated voltage and 5F capacitance costs \$15.3 while another UC with 5.4V and 1.5F costs only \$10.2. Therefore, we should consider the overall cost of the components as well as their specifications when a BMS is designed.

### C. Problem Statement

In this paper, we want to develop a BMS that enables its battery pack to supply the required power ( $P_{req}(t)$ ) for a long time. Specifically, we would like to determine the BMS operation at each time instant ( $t$ ) so as to maximize the battery life ( $L_{cycle}$ ) within tolerable voltage ( $\leq |V_r|$ ) and current range ( $\leq |I_r|$ ), which is formally expressed as:

Given the power requirements  $\{P_{req}(t)\}_{0 < t < t_{op}}$ , determine the states of control knobs for the HESS, such that  $L_{cycle}$  is maximized subject to the fixed cost without causing over-voltage ( $> |V_r|$ ) and over-current ( $> |I_r|$ ), where 0 and  $t_{op}$  are the beginning and end time instants of the battery operation, respectively. Note that the power requirements and the control knobs’ states are valid/necessary only during the EV’s operation in  $[0, t_{op}]$ . Available control knobs will be extracted by carefully considering the physical dynamics on the HESS in Section IV.

Note that  $L_{cycle}$  monotonically decreases with the increase of the cumulative amount of current according to Eq. (1). Therefore, we focus on minimization of the cumulative current ( $I_{bat}$ ) over time to maximize  $L_{cycle}$ .

### D. Cyber-physical system perspective of the HESS

Various control schemes and architectures for HESS have been proposed and studied for efficient usage of batteries. However, they have not been adopted in EVs due to their high cost. Thus, we need to develop a more efficient HESS which addresses the cost problem via integrated management exploiting existing approaches. To this end, we build a cyber-physical system (CPS) for HESS by considering all the parameters that affect discharge/charge operation beneath the HESS. We first capture the physical dynamics of HESS, and identify the effective control knobs including new control knobs which have not been identified before. Then, we propose integrated management with a relevant architecture that enhances the life of the HESS by effectively regulating the control knobs.

In the rest of the paper, we detail the cyber-physical system of HESS shown in Fig. 6. In Section IV, we explore physical dynamics when UCs supply power through a DC/DC converter. Our careful exploration of the physical side enables extraction of effective control knobs that are able to regulate the physical operation and enhance the battery life. Section V develops the management algorithms that can determine desirable control knobs yielding a long battery life based on the understanding of physical dynamics detailed in Section IV. In Section VI, we construct not only the HESS architecture which is able to regulate the control knobs, but also a unified management algorithm that can be applied to the architecture.

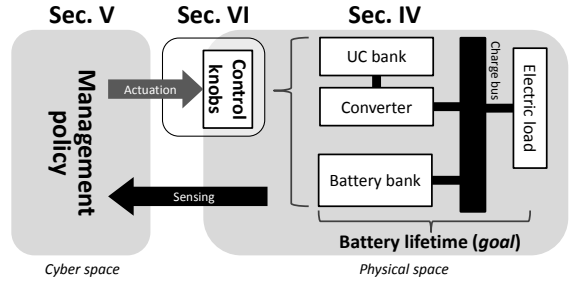


Fig. 6. CPS perspective for the design/management of the HESS

## IV. ANALYSIS OF DISCHARGE/CHARGE RATE OF A HESS

Discharge/charge rate greatly affects the battery life, and should therefore be controlled properly. Unlike the conventional battery systems, the battery discharge/charge rate can be regulated in a HESS due to UCs’ capability of controlling discharge/charge current. For example, an increase (decrease) in discharge current of UCs decreases (increases) discharge current of batteries while supplying the total required current to the electric load. In this section, we first describe how converters in the HESS operate and how they influence the discharge/charge rate of UCs. Second, we identify controllable parameters that affect the discharge/charge rate of UCs.

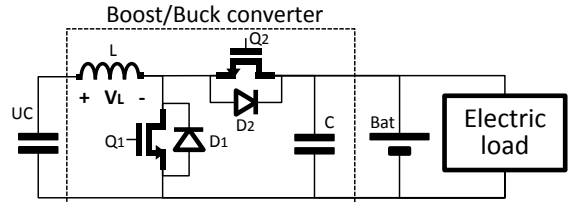


Fig. 7. A basis for the proposed HESS

### A. Circuit dynamics in the HESS

We investigate the physical dynamics of the UC-converter-battery unit shown in Fig 7 [32], because this will be the basis for our approach in the following sections. The main principle is that an inductor resists changes in current by developing a voltage ( $V_L$ ) across it which is proportional to the rate of the current change as:

$$V_L = L \frac{dI}{dt}. \quad (2)$$

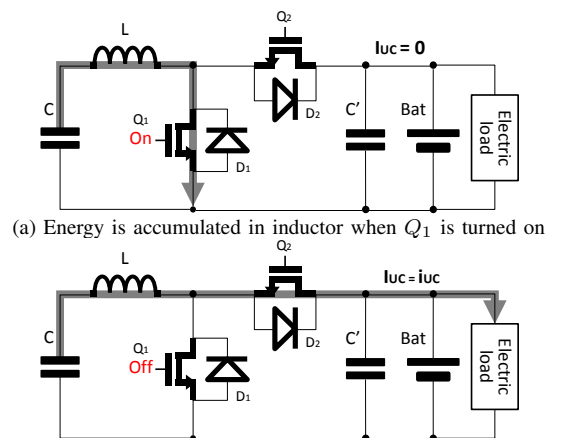


Fig. 8. Physical dynamics of the UC-converter-battery unit

When switch  $Q_1$  is closed, electron flow ( $I$ ) occurs through the inductor ( $L$ ) because output voltage of the UC drives current between terminals of the inductor. According to Eq. (2), the inductor allows the current to slowly increase by decreasing its voltage drop, and energy is accumulated in the inductor. Then, when switch  $Q_1$  is opened, current will be decreased slowly since the inductor fights abrupt changes in current. As a result, the inductor must act like a current source toward the electric load through diode  $D_2$  for a few seconds. One can expect a similar effect during recharging through  $D_1$  by controlling  $Q_2$  switch. Therefore, the converter makes charge in UCs (likewise load) transfer to the load (likewise UCs) by repeatedly switching  $Q_1$  (likewise  $Q_2$ ).

During this process, the amounts of stored and transferred energy are affected by the size of the inductor ( $L$ ) and the capacitor ( $C$ ). When  $Q_1$  is closed, the charge stored in the capacitor transfers to the inductor in the  $LC$  circuit. The differential equation of the  $LC$  circuit is

$$\frac{d^2 i_{UC}(t)}{dt^2} + \frac{1}{LC} i_{UC}(t) = 0,$$

and the solution of this differential equation is

$$i_{UC}(t) = I_p \sin\left(\frac{1}{\sqrt{LC}}t\right), \quad (3)$$

where  $I_p$  is the peak current. Note that the rate of energy transferred to the load is dominated by the size of  $L$  and/or  $C$  (from  $\frac{1}{\sqrt{LC}}$  called the *resonance frequency*). Peak current ( $I_p$ ) can be calculated based on the law of energy conservation as:

$$\begin{aligned} E_{tot} = E_C + E_L &= \frac{1}{2}LI^2 + \frac{1}{2}CV^2 \\ &= \frac{1}{2}LI_p^2 + 0 = 0 + \frac{1}{2}CV_0^2, \end{aligned} \quad (4)$$

where  $V_0$  is the initial voltage difference through the inductor. Initially, all the energy in the system is stored in the UC ( $\frac{1}{2}CV_0^2$ ) and no energy in the inductor. When  $Q_1$  is closed, the energy in UCs starts to transfer to the inductor as a form of current ( $\frac{1}{2}LI^2$ ). Because total energy in the  $LC$  circuit must be conserved, the energy and current in an inductor reach the peak current when all the energy accumulated in UCs transferred to the inductor. Eq. (4) can be modified as:

$$I_p = \sqrt{\frac{C}{L}}V_0.$$

Note that the large capacitance ( $C$ ), initial voltage of the UC ( $V_{UC}$ ) and small inductance ( $L$ ) yield a high peak current ( $I_p$ ). Finally, Eq. (3) can be re-written as:

$$i_{UC,on}(t) = \sqrt{\frac{C}{L}}V_{UC} \sin\left(\frac{1}{\sqrt{LC}}t\right). \quad (5)$$

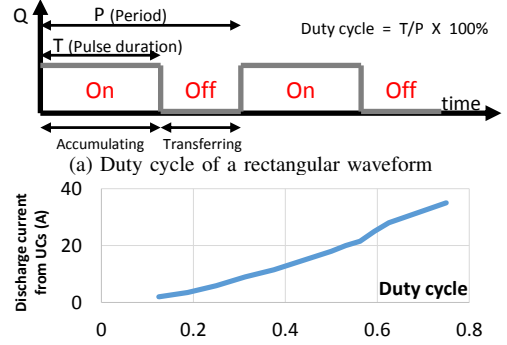
We can also expect a similar effect when  $Q_1$  is closed and write the discharge current as:

$$i_{UC,off}(t) = \sqrt{\frac{C}{L}}(V_{UC} - V_{bat}) \sin\left(\frac{1}{\sqrt{LC}}t\right), \quad (6)$$

where  $V_{bat}$  is the battery voltage.

## B. Control knobs

Eq. (5) shows parameters that should be controlled for an efficient BMS. We now present the three control knobs affecting the parameters ( $t$ ,  $L$ ,  $C$ , and  $V_{UC}$ ) in the equation, which are the keys to the development of our discharge/charge rate management to be presented in Section V.



(b) Discharge current varies with the duty cycle of converter control signal  
Fig. 10. Duty cycle as a control knob

1) *Duty cycle of signal for converter switches* ( $i_{UC}(t) = \sqrt{\frac{C}{L}}V_0 \sin(\frac{1}{\sqrt{LC}}t)$ ): To operate the converters in the HESS, we need the switching signals for  $Q_1$  and  $Q_2$  switches. The duty cycle of the signal, the ratio between the pulse duration ( $T$ ) and the period ( $P$ ), should be controlled properly, because it determines the energy accumulation period ( $T$ ) and the amount of charge moving to/from the electric load as illustrated in Fig. 9-(a). Fig. 10-(a) illustrates an example of duty cycle for the converter switches, and Fig. 10-(b) shows the discharge current variation with duty cycles. For example, when the converter accumulates more energy during each period due to an increase in the duty cycle, the system supplies more energy to the electric load.

2) *LC Configuration of the UC-converter in the UC bank* ( $i_{UC}(t) = \sqrt{\frac{C}{L}}V_0 \sin(\frac{1}{\sqrt{LC}}t)$ ): The  $LC$  configuration in the UC-converter dictates the UC's capacitance ( $C$ ), the inductor's inductance ( $L$ ) and the capacitor output voltage ( $V_0$ ) as described in Fig. 11, and then affects the form of discharge/charge current according to Eq. (5). For example, a change in current through a larger inductor (high  $L$ ) in the HESS tends to be slower as illustrated in Fig. 9-(b). Therefore, we can adaptively determine discharge/charge patterns by regulating  $V_0$ ,  $L$  and  $C$  via reconfiguration of  $LC$  circuit in the multiple UC-converters. For instance, when a UC bank's voltage ( $V_0$ ) is too low to supply the required current, we can serialize UCs in the UC bank so as to increase output voltage of the UC bank.

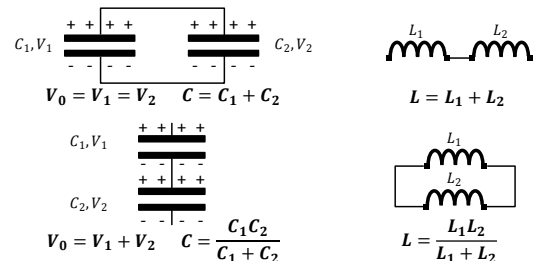


Fig. 11. Voltage, capacitance and inductance vary with the configuration

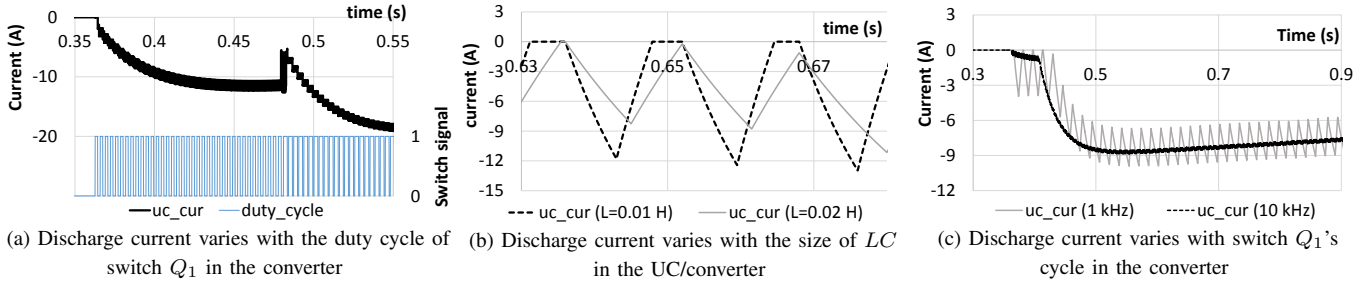


Fig. 9. Three control knobs for discharge-rate management

3) *Frequency of signal for converter switches*: Discharge/charge current fluctuations in batteries may damage batteries. For example, as shown in Fig. 9-(c), discharge current changes greatly and peak-to-peak current gets up to 4A when it is operated by a 1 kHz switch signal, whereas discharge/charge current is stable at 10 kHz switch frequency. Therefore, the converter switches should be cycled fast enough to prevent the excessive discharge/charge current fluctuations. However, the required frequency for stable discharge/charge rate varies with *duty cycle* and *LC configuration* in the UC-converters, since the form of discharge/charge current depends on them. Based on the *duty cycle* and the *LC configuration*, we then adaptively regulate the frequency of the converter input switches to protect batteries from excessive discharge/charge current variations.

## V. THE PROPOSED BATTERY DISCHARGE/CHARGE-RATE MANAGEMENT IN THE HESS

So far, we have examined circuit dynamics and control knobs that affect the discharge/charge current in the HESS. Based on them, we now develop battery discharge/charge rate management policies to extend the battery life. We first state the requirements for extending the battery life, and then develop an overall management policy.

### A. Requirements

To extend the battery life, a BMS should mitigate the discharge/charge stress. Also, to avoid fast performance degradation, we should reduce peak discharge current ( $\max(I_{bat}(t))$ ) and the amount of charge transferred to/from the electric motors as follows.

- Minimize  $\left[ \int |I_{bat}(t)| dt \right]$ .
- Minimize  $\left[ \max(I_{bat, discharge}(t)) \right]$ .
- $\left[ I_{bat, recharge}(t) = 0 \right]$ .

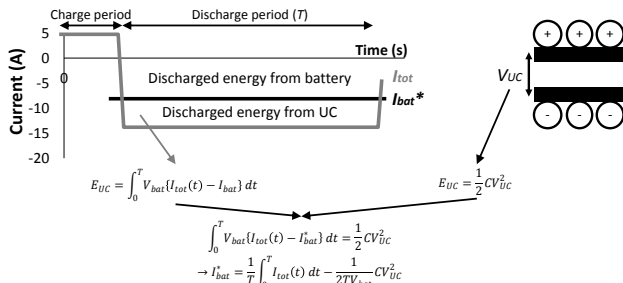


Fig. 12. Calculation of target battery current ( $I_{bat}^*$ )

To satisfy the requirements of minimizing battery discharge/charge stress, all the energy in the UC ( $E_{UC} = \frac{1}{2} CV^2$ ) should be discharged during the discharge period ( $T$ ), and the UC accumulates the charge supplied by the RBS to reduce charge stress of battery as shown in Fig. 12. If total discharge current is known through a power requirement prediction, we can calculate constant target battery discharge current ( $I_{bat}^*$ ) during the period ( $T$ ) satisfying the requirements for reducing battery discharge/charge stress. The target discharge current ( $I_{bat}^*$ ) is set to “0” if the braking system supplies charge to the battery ( $I_{tot} > 0$ ), or “ $\frac{1}{T} \int_0^T I_{tot}(t) dt - \frac{1}{2TV_{bat}} CV_{UC}^2$ ” otherwise. The following approaches in Sec. V-B are taken to make the battery current ( $I_{bat}$ ) the target battery current ( $I_{bat}^*$ ) as seen in Fig. 14.

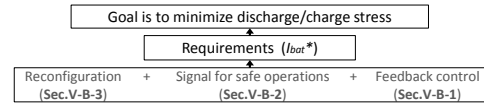


Fig. 14. Requirements and approaches

### B. Overall Management

By satisfying the requirements, we can design an efficient discharge/charge rate manager achieving a long life as seen in Fig. 14. To this end, we propose an integrated management algorithm for *duty cycle*, *frequency*, and *configuration* as illustrated in Fig. 13. Our management algorithm determines the *duty cycle* of converter switches that make target battery current ( $I_{bat}^*$ ), and *configuration* of UC-converters ( $V_{UC}$ ,  $L$  and  $C$ ) which enables the HESS to achieve the target battery discharge/charge rate ( $I_{bat}^*$ ). Meanwhile, the *frequency* for converter switches should be chosen carefully for the stable transfer of charge.

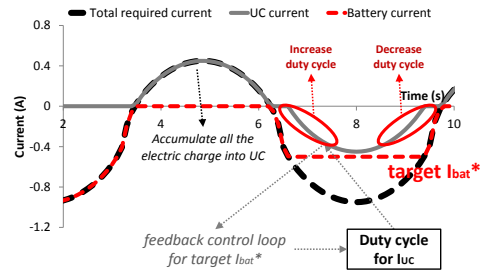


Fig. 15. Duty cycle selection

1) *Dynamic regulation of duty cycle*: To satisfy the requirements for achieving high UC utilization and moderate stress on the batteries, we set the target battery and UC current ( $I_{bat}^*$  and  $I_{UC}^*$ ). We achieve the target discharge current by regulating the discharge rate of UCs ( $I_{UC}$ ) through adaptive selection of duty cycle ( $D$ ) as follows.

In Section IV-A, we explored the discharge current when a switch is repeatedly turned “on” and “off” ( $i_{UC,on}$  and

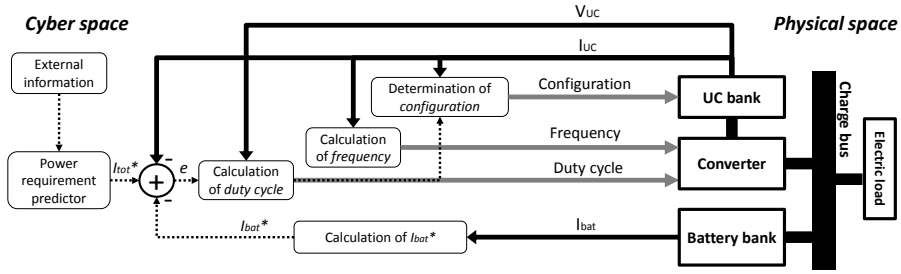


Fig. 13. A schematic diagram of discharge/charge rate management: solid black lines, solid black arrows, solid grey arrows, and black dotted arrows indicate the current flows in the physical space, sensing flows, control for the physical space, and control flows in the cyber space, respectively;  $I_{tot}^*$ ,  $I_{bat}$ ,  $I_{bat}^*$  and  $I_{UC}$  denote the total predicted discharge/charge current, the discharge/charge current of a battery, the target discharge/charge current of a battery and a UC. Based on these values, the manager regulates the control knobs (i.e., *control frequency*, *duty cycles* and *configuration* of UC-converters)

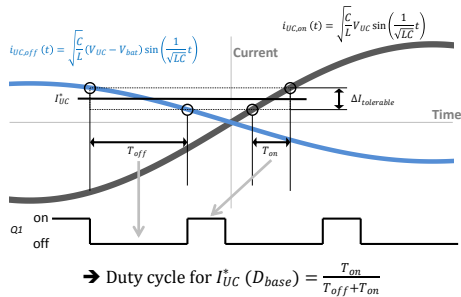


Fig. 16. Base duty-cycle calculation

**Algorithm 1** Algorithm for dynamic regulation of duty cycle (DUTY)

- 1:  $I_{bat}^* \leftarrow \text{target}(I_{bat}, C, V_{UC}, V_{bat}, T, I_{tot}^*(t));$
- 2:  $D_{base} \leftarrow (L, C, V_{UC}, V_{bat})$
- 3:  $e \leftarrow I_{bat}^* - I_{bat};$
- 4:  $e_d \leftarrow \frac{(e - e_{prev})}{\Delta t};$
- 5:  $u \leftarrow k_p \cdot e + k_d \cdot e_d; // k_p \text{ and } k_d \text{ are tuning parameters}$
- 6:  $D \leftarrow D_{base} + u;$

$i_{UC,off}$ ). By comparing the change rates of these discharge currents ( $i_{UC,on}$  and  $i_{UC,off}$ ), we can calculate the base duty cycle ( $D_{base}$ ) that can maintain the required discharge current ( $I_{UC}^*$ ). Fig. 16 and the following equation show how to calculate the base duty cycle for the target discharge current.

$$D_{base} = \frac{T_{on}}{T_{on} + T_{off}},$$

where  $T_{on}$  (likewise  $T_{off}$ ) is the time duration the UC's current  $i_{UC,on}$  (likewise  $i_{UC,off}$ ) changes up to tolerable variation ( $\Delta I_{tolerable}$ ) when the UC supplies the target current ( $I_{UC}^*$ ).

To reduce the error due to inaccuracy in voltage measurements ( $V_{UC}, V_{bat}$ ) or element sizes ( $L, C$ ), we also adopt a *PD controller* handling the difference ( $u$ ) between the target battery current ( $I_{bat}^*$ ) and the present battery current ( $I_{bat}$ ) as seen in steps 3–5 of Algorithm 1. Finally, we select the duty cycle ( $D$ ) to make the batteries supply the target discharge current ( $I_{bat}^*$ ) based on the base duty cycle ( $D_{base}$ ) and the estimation of difference ( $u$ ) between the target and actual discharge rate.

2) *Dynamic regulation of switching frequencies for converters*: To protect the batteries from current surges due to a periodically controlled converter, we control the frequencies ( $f = \frac{1}{T}$ ) of the signal for the converter switches. We repeatedly capture the peak-to-peak discharge current of UCs (peak-to-peak  $I_{UC}$ ), and regulate the frequency, achieving

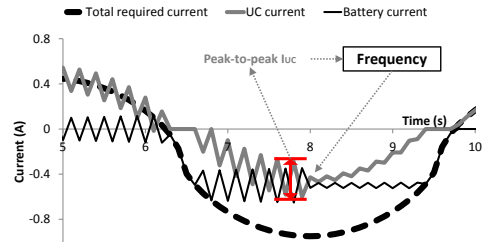


Fig. 17. Selection of frequencies for converters

**Algorithm 2** Algorithm for dynamic frequency regulation (FREQ)

- 1: **if** |peak-to-peak  $I_{UC}$ |  $\geq$  margin **then**
- 2:  $f \uparrow$
- 3: **else**
- 4:  $f \downarrow$
- 5: **end if**

the moderate discharge rate of UCs and batteries as illustrated in Fig. 17 and Algorithm 2.

3) *Reconfiguration*: To increase the voltage swing range of UC banks while maintaining the capacity of the bank, we reconfigure UC-converter dynamically. When the UC bank is already charged or supposed to be recharged from the RBS soon, we parallelize the UCs in the bank to store the charge in UCs efficiently. However, the charge would be transferred to the electric load for operating EVs, and the capacitor voltage ( $V_0$ ) would be dropped over time. Then, UC banks cannot supply required current ( $u \geq \text{margin}$ ) effectively due to lack of peak discharge current ( $I_p$  in Eq. (3)) even if the duty cycle ( $D$ ) is maximum. In this case, we restore the output voltage of UC banks to increase peak current ( $I_p$ ) by serializing the UCs. This reconfiguration enables the bank to supply the charge to the load, leading to larger voltage swing and energy capacity utilization as shown in Fig. 18. Algorithm 3 shows this process for determining whether to serialize or parallelize configuration (CFG) of the UC-converter in the HESS based on the current duty cycle ( $D$ ) and the difference between the target and actual currents ( $u$ ).

## VI. IMPLEMENTATION

So far, we have examined the circuit dynamics underlying HESSes and relevant management policies for efficient usage of UC banks. This section describes our implementation of a HESS architecture that supports the management algorithms discussed in Section V.

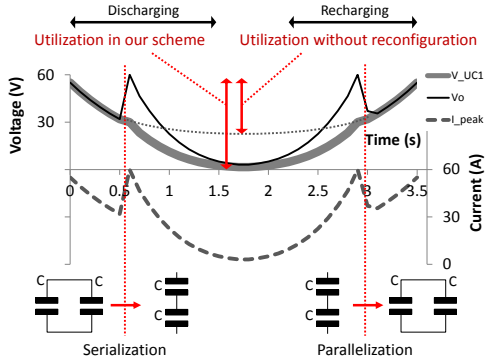


Fig. 18. Selection of HESS configuration

**Algorithm 3** Algorithm for selection of the HESS configuration (CFG)

```

1: if  $D = \max(D)$  &  $u \geq \text{margin}$  then
2:   CFG  $\leftarrow$  Series;
3: else if  $I_{bat} \leq 0$  then
4:   CFG  $\leftarrow$  Parallel;
5: else
6:   NO ACTION
7: end if

```

**A. Basic HESS architecture**

Fig. 19 shows a basic HESS architecture. Let  $N_p$  and  $N_s$  denote the number of UCs connected in parallel and series, respectively, and they are determined based on the components' physical constraints as discussed in Section III-B. For example, if an UC pack should operate at high voltage, we have to deploy a large number of UCs in series ( $N_s$ ).

**B. Reconfigurable architecture**

The discharge/charge rate of the battery and UCs is strongly coupled with the HESS topology as seen in Section IV-B2. Also, Section II-A shows the required discharge/charge rate ( $I_{tot}$ ) in a modern energy storage varies widely, necessitating various HESS configurations. An optimal topology of the UC-converter depends on states of charge in UCs and/or the required discharge/charge current, necessitating a reconfigurable HESS. Therefore, we add reconfigurability with a few additional switches on the basic architecture of a HESS as illustrated in Fig. 20.

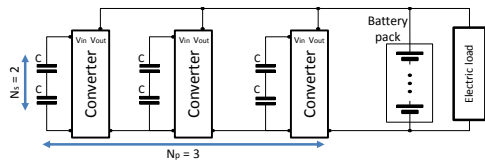


Fig. 19. Basic architecture for a HESS

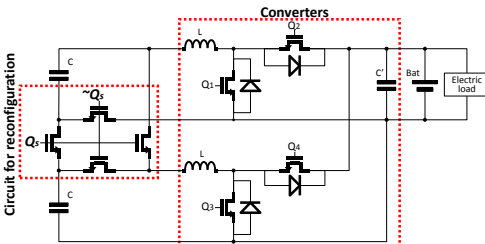


Fig. 20. Reconfigurable architecture for a HESS

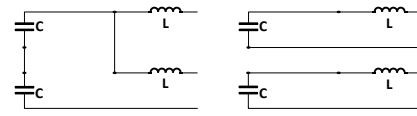


Fig. 21. Two available configurations; the left configuration is set when  $Q_s$  is turned on and the right configuration when the switch is turned off

**Algorithm 4** Algorithm for Discharge/Charge Rate Management

```

1: while 1 do
2:    $[I_{bat}, I_{UC}] \leftarrow$  current sensors;
3:    $I_{tot}^* \leftarrow$  Power requirement prediction;
4:    $[D_{Q_1, Q_2, Q_3, Q_4}, u] \leftarrow$  DUTY( $I_{tot}^*, I_{UC}, I_{bat}$ );
5:    $f_{Q_1, Q_2, Q_3, Q_4} \leftarrow$  FREQ( $I_{UC}$ );
6:   CFG  $\leftarrow$  CFG( $D, u$ );
7:   if CFG = Series then
8:      $Q_s \leftarrow 1$ ;
9:   else
10:     $Q_s \leftarrow 0$ ;
11:   end if
12:   delay( $\Delta t_{control}$ );
13: end while

```

An input of switch  $Q_s$  determines the topology as seen in Fig. 21. For example, if  $Q_s$  is opened, we can use two UC-converter units which have  $C$  capacitance and  $L$  inductance, allowing for storing a large amount of charge. When the switch  $Q_s$  is closed, UCs are serialized while inductors are parallelized, leading to decrease in not only capacitance of the UC bank ( $2C \rightarrow \frac{1}{2}C$ ) but also inductance of the inductor in the converter ( $2L \rightarrow \frac{1}{2}L$ ). Serialization of UCs can increase peak current ( $I_p$ ) due to the increased voltage ( $V_0$ ), enabling the BMS to effectively exploit UCs.

**C. Management algorithm**

The cyber part should be able to select inputs of switches ( $Q_s, Q_1, Q_2, Q_3$  and  $Q_4$ ) to satisfy the target discharge/recharge rate of batteries and UCs. Algorithm 4 describes our management policy. The main principle of our approach is to capture the charge in the UC bank temporarily and supply them to the electric load in order to reduce the battery stress. Steps 2–3 pre-process; we measure the current of UCs and battery banks, and calculate the discharge current of the next step. Steps 4–5 determine the form of cycled signal for converter switches. Algorithm 1 regulates duty cycle ( $D_{Q_1, Q_2, Q_3, Q_4}$ ) of switch signals to yield the desirable battery current for longer lifetime, and Algorithm 2 chooses the frequency ( $f_{Q_1, Q_2, Q_3, Q_4}$ ) of the signals for protecting cells from excessive current variations caused by periodically controlled ( $\Delta t_{control}$ ) converters. Steps 6–11 decide on the configuration of UC-converters (CFG) according to Algorithm 3.

**VII. EVALUATION**

We now evaluate the proposed HESS. We first introduce performance metrics for the HESS and then describe the tools and settings used for the performance evaluation. Finally, we present the evaluation results. Fig. 22 describes our evaluation process.

**A. Evaluation metrics: battery lifetime**

Lifetime is an important metric in evaluating large-scale battery systems, because it significantly affects the cost of EVs.

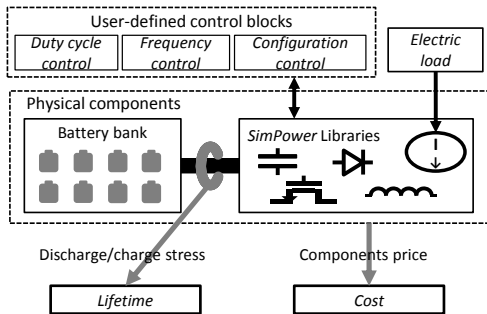


Fig. 22. Evaluation process

To evaluate the battery lifetime in the proposed HESS, we conducted extensive simulations, and recorded discharge/charge stresses. Then, we computed the battery lifetime by feeding the stress measurements into the lifetime model introduced in Section III-A. We evaluated the lifetimes of multiple systems built at the same materials cost for a fair comparison.

### B. Evaluation tools and settings

We built the several energy storage architectures by programming the control blocks and loading electric component models in a simulation tool. We then simulated different HESSes with a given electrical load using MATLAB, which is widely used for the verification of control systems [33]. During simulations, we recorded the interesting physical states to evaluate the HESSes.

1) *Electric load*: The US Environmental Protection Agency (EPA) provides “Dynamometer Drive Schedules” for standard emissions testing of driving. We used the dynamometer drive schedules as the *electric load* of an EV’s powertrain.

2) *Physical space simulation*: MATLAB is a high-level language with a numerical computing environment, developed by MathWorks. *SimPowerSystems* library in MATLAB provides electric component models and tools for modeling and simulating electrical power systems. We used the component models to implement our reconfigurable HESS architecture in Section VI. We filled in the internal parameters of the components library by using the specification of components in the website [31] for realistic simulations.

3) *Cyber space implementation*: We also implemented control blocks describing our management algorithms. We specified the inputs of the control blocks and made the blocks determine outputs via the proposed algorithms such as *duty cycle control*, *frequency control* and *configuration control*. The algorithms monitor the states of the HESS and regulate the control knobs based on the states so as to reduce the discharge/charge stress of batteries.

### C. Evaluation results

We have evaluated the following three HESS schemes:

- BASE: no ultra-capacitors;
- EX: existing HESSes introduced in Section II (the HESS with DC/DC converters);
- DRF: our HESS described in Section V (adaptive discharge/charge rate management with a reconfigurable architecture).

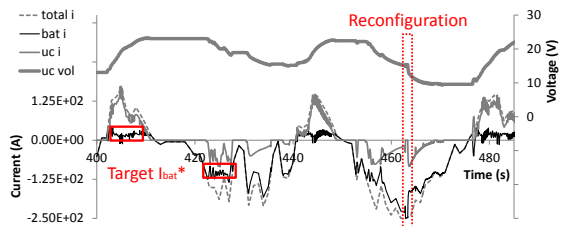


Fig. 23. Example of discharge/charge current of DRF

1) *Lifetime*: We ran simulation and extracted the discharge/charge stress of batteries for each scheme. Then, we estimated their lifetime based on the lifetime model. Table II shows the ratio of the average lifetime of DRF (and EX), to that of BASE. As shown in this table, DRF improves the lifetime by up to 153% and 37.7% over BASE and EX, respectively. We compared the discharge/charge stress to batteries under the three schemes by using the following equation.

$$\bullet \frac{1}{T} \left[ \int_0^T |I_{bat}(t)| dt \right],$$

where  $T$  is an operation period. Table III shows the battery stresses under the same workload. Compared to BASE, DRF reduces the stress by 15.9%. DRF is even better than EX in that it can reduce the discharge/charge stress by up to 5.4% than EX. This reduction of discharge/charge stress extends the lifetime under DRF.

Type	EX/BASE	DRF/BASE
Lifetime ( $N_{cycle}$ )	1.83	2.53

TABLE II. LIFETIME OF ENERGY STORAGE SYSTEMS

Type	BASE	EX	DRF
Stress of Battery	149.42	135.67	128.43

TABLE III. DISCHARGE/CHARGE STRESS OF ENERGY STORAGE SYSTEMS

2) *Energy Capacity Utilization of UCs*: Our HESS introduced in Sections V and VI includes the method to increase the utilization of energy capacity. It actually contributes to the extension of battery life, since increasing the capacity utilization decreases the discharge/charge stress of batteries. We first calculate the target battery discharge current ( $I_{bat}^*$ ) maximizing UC utilization, and the proposed management policy manipulating UCs current ( $I_{UC}$ ) to satisfy the target battery discharge current as shown in red boxes in Fig. 23. Furthermore, whenever UCs cannot supply the required current due to lack of UC bank voltage, the HESS reconfigures UC-converters to boost the voltage of UC banks to supply a sufficient amount of charge. As shown in dotted red box in Fig. 23, our HESS changes the configuration so as to supply charge effectively by allowing a larger voltage swing of the UCs.

## VIII. CONCLUSION

To meet the increasing demand to make EVs financially affordable, BMSes should be able to cope with harsh discharge/charge rate that affects the battery life significantly. A form of switch inputs (frequency and duty cycle) for converters and the HESS configuration are key control knobs for slowing

down the battery capacity degradation, since they have significant impact on the discharge/charge rate of each energy storage device in the HESS. In this paper, we have presented how to achieve efficient battery management using these control knobs. We proposed a new battery discharge/charge rate management scheme that determines, in real time, the form of input signals and the configuration of the HESS based on the analysis of their impact on the discharge/charge rate of battery cells. To realize this scheme, we also proposed the reconfigurable HESS architecture, which can select the configuration of the HESS. Our evaluation using realistic simulation has shown that the proposed HESS management makes a significant improvement of battery life without increasing cost, over a simple method often seen in the existing BMSes.

It would be interesting to improve the discharge/charge rate management based on the proposed architecture. One direction is to improve the performance of discharge/charge rate management with a power requirement prediction, since it allows BMSes to prepare for supplying or storing energy in advance [13]. Our approaches can also be used for other types of HESSes including fuel cells which have their own power and energy densities. These are matters of our future inquiry.

#### ACKNOWLEDGEMENT

The work reported in this paper was supported in part by the NSF under grants CNS-1446117 and CNS-1138200. This work was also supported by LG Chem Ltd., and Basic Science Research Program through the National Research Foundation of Korea (NRF) funded by the Ministry of Science, ICT & Future Planning (NRF-2014R1A1A1035827).

#### REFERENCES

- [1] J. TROP and D. CARDWELL, "Tesla plans 5 billion battery factory for mass-market electric car," Feb 2014. [Online]. Available: [http://www.nytimes.com/2014/02/27/automobiles/tesla-plans-5-billion-battery-factory-for-mass-market-electric-car.html?\\_r=0](http://www.nytimes.com/2014/02/27/automobiles/tesla-plans-5-billion-battery-factory-for-mass-market-electric-car.html?_r=0)
- [2] Electropaedia. Battery life (and death). [www.mpoweruk.com/life.htm](http://www.mpoweruk.com/life.htm).
- [3] D. Linden and T. Reddy, *Handbook of batteries*, 3rd ed. McGraw-Hill, 2002.
- [4] H. Kiehne, *Battery Technology Handbook*, 2nd ed. CRC Press, 2003.
- [5] M. Majima, S. Ujiie, E. Yagasaki, K. Koyama, and S. Inazawa, "Development of long life lithium ion battery for power storage," *Journal of Power Sources*, vol. 101, no. 1, pp. 53 – 59, 2001.
- [6] S. S. Choi and H. S. Lim, "Factors that affect cycle-life and possible degradation mechanisms of a li-ion cell based on licoo2," *Journal of Power Sources*, vol. 111, no. 1, pp. 130 – 136, 2002.
- [7] E. Faggioli, P. Rena, V. Danel, X. Andrieu, R. Mallant, and H. Kahlen, "Supercapacitors for the energy management of electric vehicles," *Journal of Power Sources*, vol. 84, no. 2, pp. 261 – 269, 1999.
- [8] P. Rodatz, G. Paganelli, A. Sciarretta, and L. Guzzella, "Optimal power management of an experimental fuel cell/supercapacitor-powered hybrid vehicle," *Control Engineering Practice*, vol. 13, no. 1, pp. 41 – 53, 2005.
- [9] R. Carter and A. Cruden, "Strategies for control of a battery/supercapacitor system in an electric vehicle," in *Power Electronics, Electrical Drives, Automation and Motion, 2008. SPEEDAM 2008. International Symposium on*, June 2008, pp. 727–732.
- [10] P. Thounthong, V. Chunkag, P. Sethakul, S. Sikkabut, S. Pierfederici, and B. Davat, "Energy management of fuel cell/solar cell/supercapacitor hybrid power source," *Journal of Power Sources*, vol. 196, no. 1, pp. 313 – 324, 2011.
- [11] M. Ortuzar, J. Moreno, and J. Dixon, "Ultracapacitor-based auxiliary energy system for an electric vehicle: Implementation and evaluation," *Industrial Electronics, IEEE Transactions on*, vol. 54, no. 4, pp. 2147–2156, Aug 2007.
- [12] C. Chan and K. Chau, "An overview of power electronics in electric vehicles," *Industrial Electronics, IEEE Transactions on*, vol. 44, no. 1, pp. 3–13, Feb 1997.
- [13] E. Kim, J. Lee, and K. G. Shin, "Real-time prediction of battery power requirements for electric vehicles," in *ACM/IEEE 4th International Conference on Cyber-Physical Systems (ICCP13)*, Philadelphia, PA, Apr 2013.
- [14] Y. Gao, L. Chen, and M. Ehsani, "Investigation of the effectiveness of regenerative braking for ev and hev." SAE International, 08 1999.
- [15] Y. Gao and M. Ehsani, "Electronic braking system of ev and hev—integration of regenerative braking, automatic braking force control and abs." SAE International, 08 2001.
- [16] H. Gao, Y. Gao, and M. Ehsani, "Design issues of the switched reluctance motor drive for propulsion and regenerative braking in ev and hev." SAE International, 08 2001.
- [17] C. Lv, J. Zhang, Y. Li, and Y. Yuan, "Regenerative braking control algorithm for an electrified vehicle equipped with a by-wire brake system." SAE International, 04 2014.
- [18] Y. Kim, S. Park, Y. Wang, Q. Xie, N. Chang, M. Poncino, and M. Pedram, "Balanced reconfiguration of storage banks in a hybrid electrical energy storage system," in *Computer-Aided Design (ICCAD), 2011 IEEE/ACM International Conference on*, Nov 2011, pp. 624–631.
- [19] A. Khaligh and Z. Li, "Battery, ultracapacitor, fuel cell, and hybrid energy storage systems for electric, hybrid electric, fuel cell, and plug-in hybrid electric vehicles: State of the art," *Vehicular Technology, IEEE Transactions on*, vol. 59, no. 6, pp. 2806–2814, July 2010.
- [20] J. Cao and A. Emadi, "A new battery/ultracapacitor hybrid energy storage system for electric, hybrid, and plug-in hybrid electric vehicles," *Power Electronics, IEEE Transactions on*, vol. 27, no. 1, pp. 122–132, Jan 2012.
- [21] S. Park, Y. Kim, and N. Chang, "Hybrid energy storage systems and battery management for electric vehicles," in *Design Automation Conference (DAC), 2013 50th ACM / EDAC / IEEE*, May 2013, pp. 1–6.
- [22] A. Pesaran. (2009) Ultracapacitor applications and evaluation for hybrid electric vehicles. [Online]. Available: <http://www.nrel.gov/vehiclesandfuels/energystorage/pdfs/45596.pdf>
- [23] E. Kim, J. Lee, and K. G. Shin, "Real-time battery thermal management for electric vehicles," in *ACM/IEEE 5th International Conference on Cyber-Physical Systems (ICCP14)*, Berlin, Germany, Apr 2014.
- [24] D. Zhang, B. Haran, A. Durairajan, R. White, Y. Podrazhansky, and B. Popov, "Studies on capacity fade of lithium-ion batteries," *Journal of Power Sources*, vol. 91, no. 2, pp. 122 – 129, 2000.
- [25] P. Ramadass, B. Haran, R. White, and B. N. Popov, "Mathematical modeling of the capacity fade of li-ion cells," *Journal of Power Sources*, vol. 123, no. 2, pp. 230 – 240, 2003.
- [26] G. Ning, B. Haran, and B. N. Popov, "Capacity fade study of lithium-ion batteries cycled at high discharge rates," *Journal of Power Sources*, vol. 117, no. 1 - 2, pp. 160 – 169, 2003.
- [27] R. Spotnitz, "Simulation of capacity fade in lithium-ion batteries," *Journal of Power Sources*, vol. 113, no. 1, pp. 72 – 80, 2003.
- [28] G. Ning, R. E. White, and B. N. Popov, "A generalized cycle life model of rechargeable li-ion batteries," *Electrochimica Acta*, vol. 51, no. 10, pp. 2012 – 2022, 2006.
- [29] A. Millner, "Modeling lithium ion battery degradation in electric vehicles," in *Innovative Technologies for an Efficient and Reliable Electricity Supply (CITRES), 2010 IEEE Conference on*, Sept 2010, pp. 349–356.
- [30] Ampacity. [Online]. Available: <http://en.wikipedia.org/wiki/Ampacity>
- [31] Digikey. [Online]. Available: <http://www.digikey.com/>
- [32] S. Pay and Y. Baghzouz, "Effectiveness of battery-supercapacitor combination in electric vehicles," in *Power Tech Conference Proceedings, 2003 IEEE Bologna*, vol. 3, June 2003, pp. 6 pp. Vol.3–.
- [33] MathWorks. Matlab. <http://www.mathworks.com/>